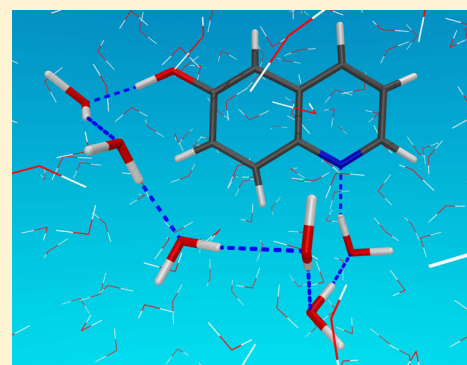


## Water Wires in Aqueous Solutions from First-Principles Calculations

Gül Bekçioğlu,<sup>†,‡</sup> Christoph Allolio,<sup>‡,§</sup> and Daniel Sebastiani<sup>\*,‡</sup><sup>†</sup>Physics Department, Freie Universität Berlin, Arnimallee 14, 14195 Berlin, Germany<sup>‡</sup>Institut für Chemie, Martin-Luther-Universität Halle-Wittenberg, Von-Danckelmann-Platz 4, 06120 Halle (Saale), Germany<sup>§</sup>Institute of Organic Chemistry and Biochemistry, Academy of Sciences of the Czech Republic, Flemingovo nám 2, CZ-16610 Prague 6, Czech Republic

## Supporting Information

**ABSTRACT:** We elucidate the concept of water wires in aqueous solutions in view of their structural and dynamical properties by means of first-principles molecular dynamics simulations. We employ a specific set of hydroxyquinoline derivatives (heteroaromatic fluorescent dyes) as probe molecules that provide a well-defined initial and final coordinate for possible water wires by means of their photoacid and photobase functionalities. Besides the geometric structure of the hydrogen bond network connecting these functional sites, we focus on the dependence of the length of the resulting water wire on the initial/final coordinates determined by the chromophore. Special attention is devoted to the persistence of the wires on the picosecond time scale and their capability of shifting the nature of the proton transfer process from a concerted to a stepwise mechanism. Our results shed light on the long debate on whether water wires represent characteristic structural motifs or transient phenomena.



## 1. INTRODUCTION

A protic solvent such as water often plays a crucial role in proton transfer reactions due to its ability to form an extended hydrogen bonded network.<sup>1–8</sup> The specific interaction of the hydrogen bond network of water with solvated compounds influences the whole reaction path by stabilizing the reaction intermediates and products via lowering of reaction barriers. In this regard, there is an ongoing debate on the ability of water to form a persistent hydrogen bonded chain (i.e., a water wire) through which the transport of a proton can occur. Water wires have been postulated in a number of studies dealing with proton transport in biological systems,<sup>9–11</sup> including the proton pump protein bacteriorhodopsin,<sup>12</sup> green fluorescent protein,<sup>13,14</sup> carbonic anhydrase,<sup>15</sup> and gramicidin A.<sup>16</sup> It remains debatable whether such water wires also exist for proton transfer in *bulk* water, i.e., without strong outer confinement.

Organic fluorescent bifunctional chromophores have a wide range of applications as molecular probes in various areas.<sup>17–20</sup> In this regard, bifunctional heteroaromatic molecules, hydroxyquinolines (HQs) and its derivatives, have been extensively studied due to their fundamental and practical features.<sup>21–32</sup> Two members of this family, 6- and 7HQ probe molecules, provide both proton donor and acceptor groups at well-defined positions, to which a water wire may be engaged (see Figure 1). Such a well-defined proton transfer pathway is difficult to observe directly inside a protein. Therefore, HQs can be seen as a model system to observe the properties of hydrogen bonded wires. HQs exhibit large changes in acidity/ $pK_a$  properties upon electronic excitation. Photoacidity/-basicity is the result of intramolecular changes in the electronic structure

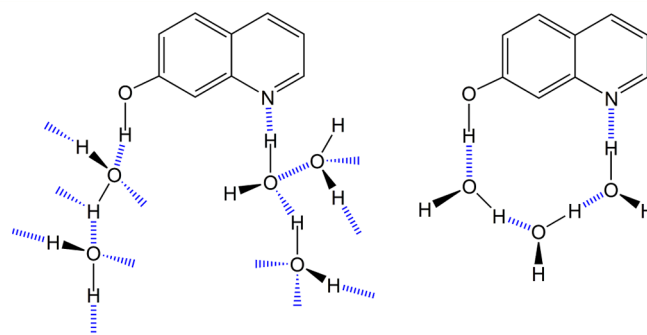


**Figure 1.** Possible solute–solvent interactions between 7HQ and water molecules. Independent water molecules hydrating donor/acceptor sites are on the left side, while the water wire engaging the donor/acceptor sites is on the right side.

compared to the situations in the electronic ground state. The excited states of HQ and its derivatives have been examined in different solvents both experimentally and computationally by several groups including our group.<sup>33–40</sup> In the previous computational studies on 6- and 7HQ, most simulations start with a predefined arrangement of an isolated cluster of H-bonded solvent molecules, and then perform *ab initio* calculations of reaction barriers for proton/hydroxide ion transfer in the excited state. In these situations, the predefined H-bonded network represents a well-defined pathway for proton

Received: December 5, 2014

Revised: February 17, 2015

Published: February 25, 2015

transport, and the pathway obtained upon photoexcitation necessarily follows this trajectory. On the experimental side, HQs in solution have been studied with transient electronic spectroscopy with time-resolved fluorescence measurements.<sup>21–29,41</sup> These experiments showed that fluorescence generated by the photoexcitation of 7HQ in water and methanol solutions reveals two rise components, concluding that the solute exists in the solution in two distinct states of solvation depicted in Figure 1.<sup>29,42–44</sup> These results suggest two corresponding processes:

- first a fast process which is accompanied by the intrinsic proton transfer through a solvent wire with an optimal configuration existing already at the moment of excitation
- a slow process starting from solvent reorganization to form a solvent wire with optimal configuration, which accordingly undergoes proton transfer rapidly

Although in the experiments no explicit evidence for water wires mediating proton transfer has been found, the possibility of the presence of such wires is often assumed as a characteristic motif of the hydrogen bond network, and used as a basis for the understanding of protonation dynamics pathways. Therefore, detailed information on the ground state solvation is required in the first place, prior to the excited state proton transfer reactions.<sup>45</sup> Recently, the ground state proton transfer dynamics of 7HQ has been studied by Jang and co-workers with configurational optimization in a hydrogen bonded alcohol wire.<sup>46</sup>

In the present paper, we elucidate the relationships between local hydrogen bonding structure and picosecond time-resolved fluorescence experiments. We investigate the ground state aqueous solvation of 6- and 7HQ by means of first-principles molecular dynamics simulations in the condensed phase. Being complementary to experiment, ab initio molecular dynamics can elucidate the microscopic details of the aqueous solvation dynamics in terms of correlation between microscopic configurations and spectroscopic parameters. In particular, we deal mainly with the microscopic details of the water configurations in terms of local structural motifs such as water wires between the polar sites of the probe molecules. We aim to understand the water reorganization to form water wires with optimal configuration that takes place prior to the excited state proton transfer process. Consequently, we hope to support the interpretation of experimental results in model systems, in view of transferring this knowledge to more complex biomolecular systems which exhibit similar processes, e.g., ion channel proteins.

**1.1. Computational Details.** The molecular dynamics were staged in a cubic, periodic box with a side length of about 21.58 Å with 6HQ:340 H<sub>2</sub>O and a side length of 21.45 Å with 7HQ:341 H<sub>2</sub>O at a density of  $d = 1.0$  g/cm<sup>3</sup>. The solvation boxes are thermostated first for 12 ps, using a Nosé–Hoover thermostat with a time constant of 50 fs at a temperature of 350 K and then continued 18 ps of a run with a time constant of 600 fs for ground state for both systems. With the increase in temperature, we hope to counter overstructuring effects, found in water simulations at lower temperature.<sup>47</sup> In addition, we used the DFT-D2 dispersion corrections<sup>48</sup> to account for dispersion effects.

For all calculations, we used the GPW<sup>49</sup> scheme as implemented in the CP2K<sup>50</sup> software package. The BLYP functional was used with a TZVP valence basis set,<sup>51</sup> Goedecker<sup>52</sup>

potentials, and a 350 Ry plane-wave cutoff. We used restricted Kohn–Sham DFT and a time step of 0.5 fs for the ground state calculations. The total length of ab initio trajectories used was 110 ps.

All DFT based static electronic structure calculations were carried out by using the Gaussian 09 program.<sup>53</sup> The conventional DFT calculations using the hybrid exchange–correlation functional B3LYP<sup>54</sup> were performed in the gas phase and in the presence of the CPCM model.<sup>55</sup> The basis set was TZVP for these calculations.

**1.2. Hydrogen Bond Definition.** We define a hydrogen bond by a combined criterion involving the oxygen–oxygen distance and the O–H–O angle between water molecules. Our choice was  $r_{\text{OO}} < 3.5$  Å,  $(\text{O}_2; \text{O}_1; \text{H}_1) < \pi/6$ , which is a common definition.<sup>56</sup> In addition to that, 2.45 Å is used as the sole criterion for the nitrogen–hydrogen bond (see the Supporting Information).

## 2. RESULTS AND DISCUSSION

**2.1. Conformation of Aqueous Solvated 6- and 7-Hydroxyquinolines.** Two spatial arrangements available to HQs, shown in Figure 2 by rotation of the hydroxyl group

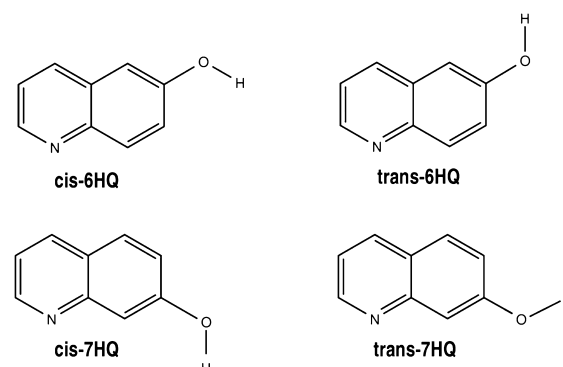


**Figure 2.** Structures of 6- and 7HQs with their rotational conformations of the hydroxyl group.

with respect to the nitrogen atom, are called cis and trans conformations, in which the hydroxyl O–H bond points down and up, respectively. We confirmed the coexistence of cis and trans conformers of 6- and 7HQs in their ground state by means of first-principles calculations. The full structure optimization calculations were performed in the vacuum and aqueous solution without any symmetry constraint. Solvation effects were captured by the conductor polarized continuum model.

The trans-7HQ is found to be 5.1 and 1.8 kJ mol<sup>−1</sup> less stable than cis-7HQ in the vacuum and the presence of implicit solvent medium, respectively. In contrast, the trans-6HQ is found to be more stable in energy than cis-6HQ by 1.7 and 1.6 kJ mol<sup>−1</sup> in the vacuum and presence of implicit solvent, respectively. It should be noticed that, under implicit aqueous solvation, the energy difference between the two rotomers is significantly below  $k_B T$  (at  $T \sim 300$  K). This indicates that HQs arrange into fast rotational isomerization among the energetically approachable conformations rather than remaining rarely immobilized in a single conformation. Furthermore, in the condensed aqueous solvation of the 6- and 7HQ, cis and trans rotamers are isoenergetic and will therefore be indistinguishable in room temperature experiments.

In order to observe the conformational isomerization in an actual molecular dynamics trajectory, we started runs for both 6- and 7HQ in the cis conformation at 350 K. In both cases, we indeed detected the geometric isomerization to the trans conformation within a simulation period of 14 and 6 ps for 6- and 7HQ, respectively.

**2.2. Existence of Water Wires.** The existence and the stability of the hydrogen bond network that connects the donor and acceptor sites of a photoacid/-base is an ongoing matter of debate.<sup>1–6,57</sup> Figure 3 shows an example of such a water wire

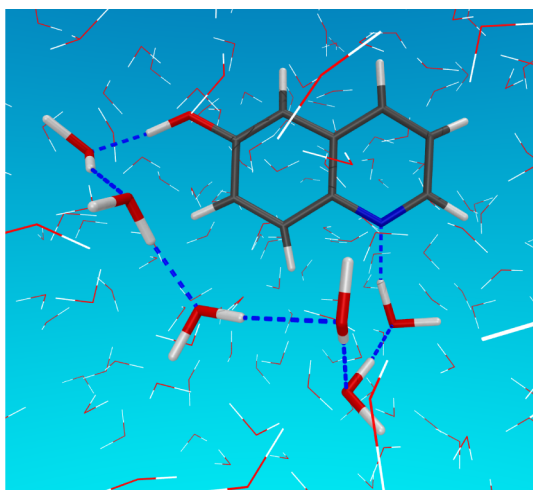


**Figure 3.** Snapshot from the MD trajectory of cis-6HQ with the water wire between proton donor and acceptor sites.

configuration. In liquid bulk water at ambient temperature, the hydrogen bond network has only a very short lifetime and its autocorrelation function is typically relaxed within a few picoseconds.<sup>58,59</sup> It should be noted here that the latter is certainly also a question of the definition of the time scale at which a water wire is considered stable. Here, we address this aspect by focusing on the existence of a reactive solute–water wire complex at a given moment (at the moment of excitation), and their persistence for a typical duration of a proton exchange reaction. The alternative scenario would be that the proton exchange trajectories mostly involve pathways that had not existed at that time.

We have computed the spatial distribution function (SDF) of water oxygen atoms between the polar sites of the probe molecules from our ab initio MD simulations (see the Supporting Information).<sup>60</sup> SDFs can provide the three-dimensional information on the location of water oxygen atoms, and therefore contain essential details about the spatial positions of water molecules interacting with HQs. These water oxygen atom densities are shown in Figure 4, which shows the most likely positions of water oxygen atoms (red clouds). Parts a and b show results for cis- and trans-7HQ, while parts c and d show the cis- and trans-6HQ, respectively. In general, these maps show that the water oxygen atoms are well localized in the hydrophilic regions of the chromophores, as expected. This indicates a strong structure-inducing effect of the HQ hydroxyl group and nitrogen atom, and water molecules in their immediate vicinity. Further than that, there are additional high-density clouds at specific locations between donor/acceptor sites which illustrate that the structure-enhancing effect clearly goes beyond the directly hydrogen bonding water molecules. The resulting pattern of high-oxygen-density clouds follows a

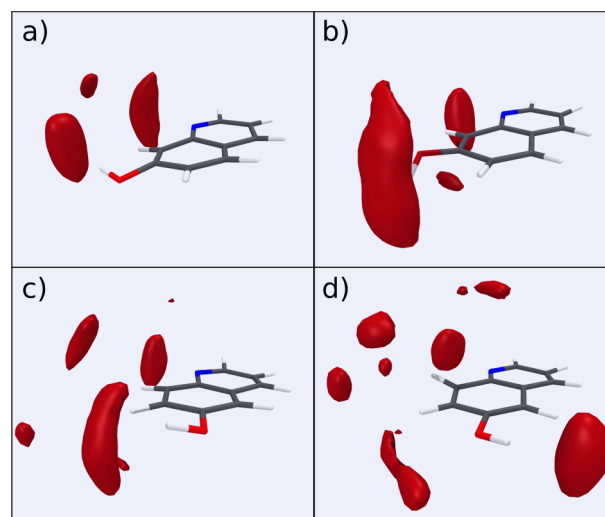


**Figure 4.** Spatial distribution functions of water oxygen atoms (red surface) around and between the hydroxyl group and nitrogen atom of (a) cis-7HQ, (b) trans-7HQ, (c) cis-6HQ, (d) and trans-6HQ.

specific path between donor/acceptor sites, which represents a consistent signature of a possible connected water wire.

**2.3. Hydrogen Bond Network Dynamics.** **2.3.1. Persistence of Water Wires.** The concept of water wires intrinsically raises the question of the persistence of an extended H-bond network of water molecules for characteristic time scales, e.g., those on which a proton exchange occurs. We address this aspect by determining the evolution of the hydrogen bonded network between polar sites of the probe molecules. We computed the number of hydrogen bonded water molecules which are connecting directly the nitrogen atom and hydroxyl group of HQs for each snapshot of our ab initio molecular dynamics trajectories (see the Supporting Information).

The occurrence of these water wires of cis- and trans-6- and 7HQs is consolidated in the histograms shown in Figure 5. The histograms thus show the probability of finding water wire consisting of a given number of water molecules connecting the polar sites of the probe molecules. Figure 5 indicates that the chemical variation (6- and 7HQ) and hydroxyl group conformation lead to characteristic changes in the distribution of the water wire pattern. For cis-7HQ there is a preference toward a typical length of three to four water molecules, while, for the trans-7HQ, on the other hand, a water wire of six molecules represents the dominant motif. This result is consistent with previous combined spectroscopic and total energy calculations of the 7HQ·(H<sub>2</sub>O)<sub>2</sub> complex,<sup>31</sup> where a water wire of two to three molecules was found to be crucial for the microscopic description of solvation and proton transfer reactions.

A water wire of six molecules is the length for the cis-6HQ. However, it is not as frequent as the one with eight water molecules. For the trans-6HQ, very few water wires composed of 5–7 molecules are observed; the typical length is rather 9–11 waters. Thus, conformational isomerization and chemical variation of the donor/acceptor sites on the probe molecules have a strong effect on the length of the resulting water wires. While a translation of the hydroxyl donor group by one carbon site yields almost a doubling in the length (4 → 8 and 6 → 11), the geometric isomerization results typically in an extension by only two water molecules.

**2.3.2. Wires in Bulk Water versus HQ-Terminated Water Wires.** Another interesting objective here is to establish an



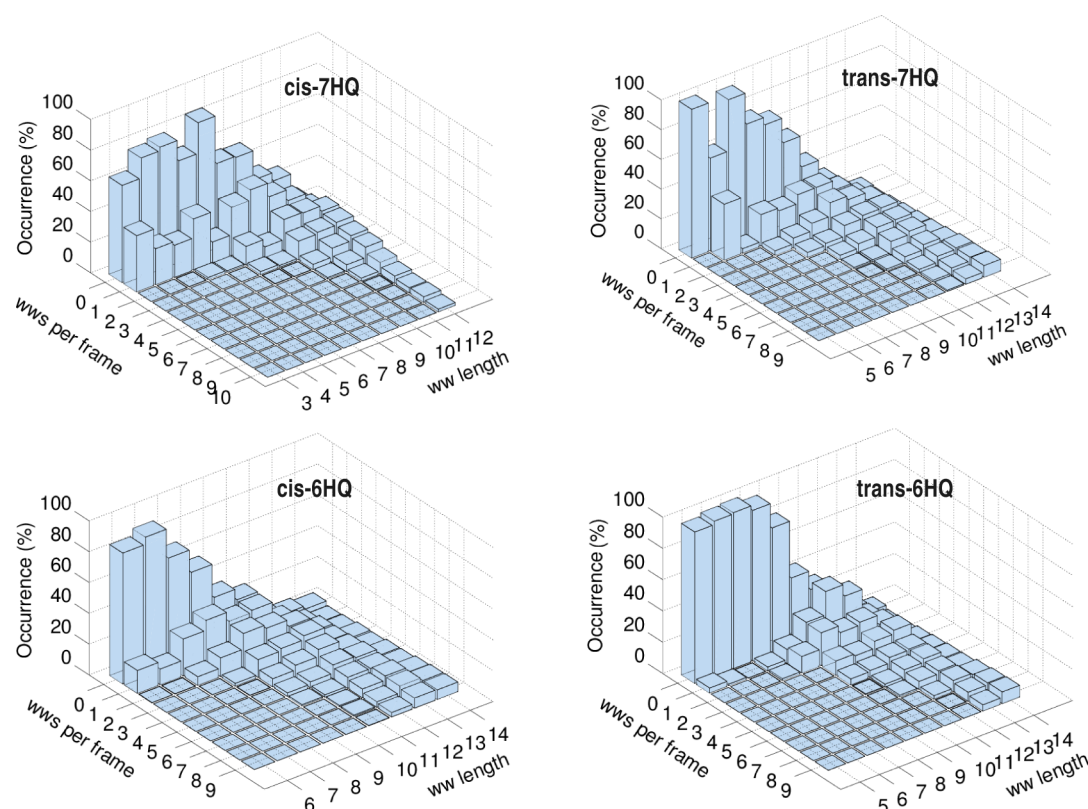


**Figure 5.** Occurrence of water wires (WWs) terminating at both the hydroxyl group and nitrogen of HQs.

atomistic comparison between lifetimes of water wires in bulk water and water wires of the same length connecting between the donor and acceptor sites of HQs. For such a comparison, we introduce here an autocorrelation function for the water wires as

$$C_{ww}^k(t) \equiv \frac{1}{\langle \eta_i^k(t_0) \rangle^2} \langle \eta_i^k(t_0 + t) \cdot \eta_i^k(t_0) \rangle \quad (1)$$

where  $\langle \dots \rangle$  denotes an average over all water wires of a given length  $k$ .  $\eta_i^k(t)$  is a water wire population descriptor for a water wire of length  $k$ .  $i$  is defined as an index to count the number of existing water wires of a given length  $k$  in each frame. Specifically,  $\eta_i^k(t) = 1$  if a tagged loop-free directed hydrogen bonded path of length  $k$  exists at time  $t$  and  $\eta_i^k(t) = 0$  otherwise. The scalar product reduces to the number of water wires present at time  $t_0$  and  $t$  simultaneously. It is important to note here that  $C_{ww}^k(t)$  is insensitive to temporary interruptions of water wires. We have used the same geometric criteria to define the hydrogen bonds between two water molecules as described in the previous section. In order to compare the water wires in bulk, we have computed water wire autocorrelations according to eq 1. For the bulk fraction of our simulation box, we used a spherical cutoff of 5 Å around the HQs, corresponding to the first peak of the radial distribution function  $g_{\text{CO}}(r)$  between the carbon atom of the HQs and the oxygen atom of water (see the Supporting Information). Complementary to this, we computed the wires in bulk water with a fixed end-to-end distance cutoff of 5 Å for cis-7HQ.

In Figure 6, we plotted the water wire autocorrelation function as a function of  $k$ . We found that the dynamics of bulk water wires substantially differs from the dynamics of water wires connecting the acidic and basic sites of cis-7HQ. Similar

observations are met with other HQs which are reported in the Supporting Information. In the bulk, the water wire lifetime decreases linearly with increasing number of water molecules (see the Supporting Information). However, there is no such trend for the water wires connecting the donor and acceptor sites of cis-7HQ. It is well evident in Figure 6 that water wires with length  $k = 3$  and  $k = 6$  decay much slower and nonexponentially. Note that the water wire length  $k = 6$  topology is accompanied by the same water molecules which form the water wire length  $k = 3$ . This surprising observation indicates that a considerably more stable HB network arrangement is achievable with water of these “magic” lengths.

To verify this interpretation, we have computed the water HB autocorrelation function within the vicinity of the first hydration shell of carbon atoms of HQs (4 Å) and outside of these regions.

$$C_{\text{HB}}(t) \equiv \frac{1}{\langle h(t_0) \rangle^2} \langle h(t_0 + t) \cdot h(t_0) \rangle \quad (2)$$

For this autocorrelation function, we used the same HB criterion as before. Again,  $h(t)$  is unity when two tagged molecules are hydrogen bonded at time  $t$  and is  $h(t) = 0$  otherwise. This function  $C_{\text{HB}}(t)$  represents the conditional probability that a HB remains intact for a time  $t$ , given it was intact at time  $t_0$ . Again,  $C_{\text{HB}}(t)$  ignores temporary breaking of HB.

In Figure 7, we found slightly slower decay of  $C_{\text{HB}}(t)$  in the vicinity of the first hydration shell which indicates the kosmotropic effect of the internal hydrophobic interface around the aromatic ring of HQ, stabilizing the water wires and retarding water reorientation dynamics.<sup>8,10,61</sup> This is consistent with recent work by Laage and co-workers, where it was shown

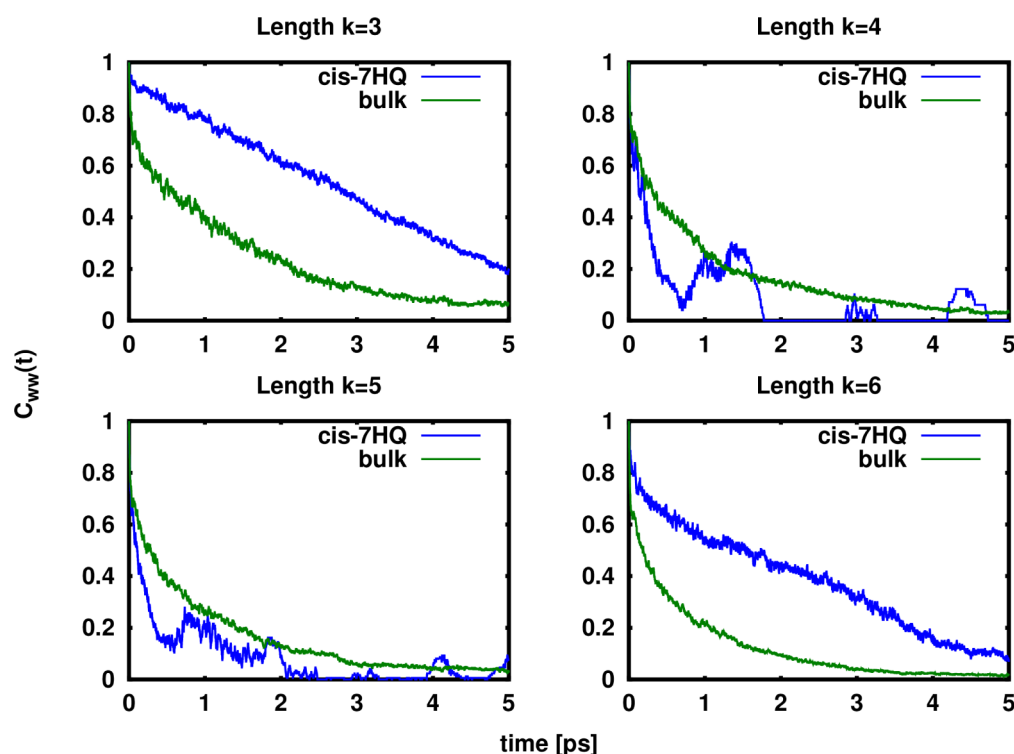


**Figure 6.** Water wire autocorrelation functions for water wires connecting the active sites of cis-7HQ (blue curve) and wires in bulk (green curve). Decays of the hydrogen bond autocorrelation functions are computed by averaging over 250 and 1000 random starting points for bulk and cis-7HQ water wires, respectively.

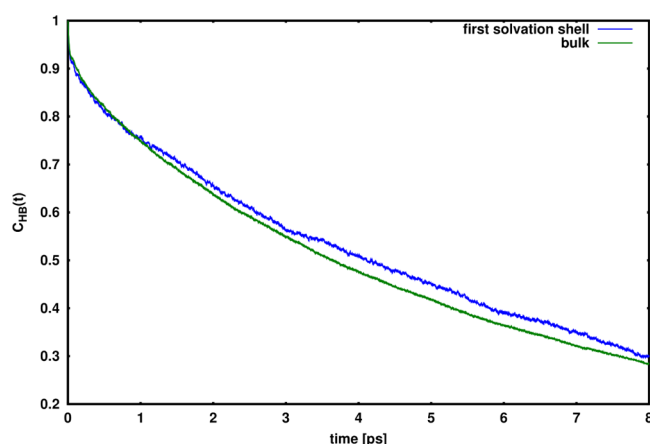


**Figure 7.** Hydrogen bond autocorrelation functions for hydrogen bonds between water for bulk water molecules (green curve) and within a distance of 4 Å of cis-7HQ (blue curve). Decays of the hydrogen bond autocorrelation functions are computed by averaging over 100 random starting points.

that the HB exchange (water rotation) process slowed down due to the excluded volume effect by the hydrophobic solute.<sup>10,62</sup> Therefore, the short water wires which are formed in the first solvation shell of HQs are more persistent with respect to the longer ones.

**2.3.3. Water Wires and Proton Exchange Pathways.** The number of water molecules in a water wire between two active sites (here, proton donor and acceptor sites of the photoacid) have a considerable influence on the nature of the proton transfer mechanism. In particular, the proton can in principle follow either a stepwise reaction dynamics or alternatively a

concerted transfer mechanism.<sup>63–71</sup> Concerted mechanisms likely occur for smaller proton transport distances, and a change into sequential transfer then is anticipated when the proton transport distance increases. This striking dynamical activity could also be driven partly by the ability of the water wires to undergo collective compressions with the presence of an excess proton.<sup>70,71</sup> In addition to that, oxygen–oxygen separations are also clearly related to the energy barrier for proton transfer. Shortening the oxygen–oxygen distance decreases the energy barrier for proton transfer.

To relate the concerted mechanism to such structural features of water wires, we have calculated the maximum oxygen–oxygen distance for the suitable water wires of length  $k = 3, \dots, 6$  of cis-7HQ. Figure 8 shows these short water wire configurations with their maximum oxygen–oxygen distances. We observe a similar phenomenon as that for the hydrogen bond network autocorrelation function: For water wires of “magic” length  $k = 3$  and  $k = 6$ , the distribution is somewhat sharper peaked at its maximum of 2.9–3.0 Å. In turn, for  $k = 4$  and  $k = 5$ , the long-distance-tails (i.e., where the maximum O–O distance reaches values above 3.0 Å) is more pronounced. This finding supports the hypothesis of an increased stability of water wires of length  $k = 3$  and  $k = 6$ , and further an increased likelihood of concerted proton transfer processes. Consequently, these water wires would be more stabilized by the presence of an excess proton allowing the concerted proton transfer event for cis-7HQ.<sup>40</sup>

On the other hand, in the stepwise process, stable  $\text{H}_3\text{O}^+$  (or  $\text{OH}^-$ ) intermediates will exist at intermediate periods of time (longer than vibrational modes but shorter than the total transfer duration), while the concerted transport reaction is characterized by their absence. On the other hand, it was known in a study of protonated linear chains of water

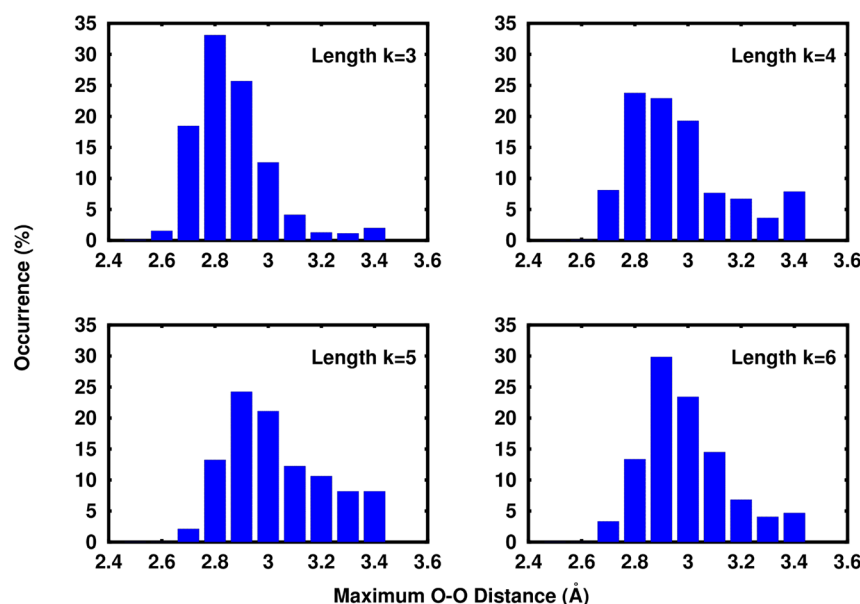


**Figure 8.** Histogram of the maximum oxygen–oxygen distances along water wires terminating at both the hydroxyl group and nitrogen of *cis*-7HQ.

molecules that proton transfer along the chain is an extremely fast process, occurring in subpicosecond time scales.<sup>72,73</sup> In such a short linear chain of water molecules, the translocation mechanism of the proton was found to be neither a concerted mechanism nor a result of a single proton hopping along the chain. The translocation process rather involved a series of semicollective motion during which rapid fluctuations of the hydrogen bond lengths along with reorganizations of water molecules are observed.<sup>74–77</sup>

So far, experimental work also could not give a conclusive dependence between the length of a water wire and the nature of the corresponding proton transfer reaction;<sup>29,78,79</sup> only the presence and absence of vibrational signals of intermediates is observable experimentally. Combining our present results with additional previous molecular dynamics simulations<sup>40,63–68</sup> and femtosecond transient IR experiments,<sup>5,78</sup> we can now conclude that a real concerted mechanism for proton conduction along a persistent water wire can only happen for water wires of four molecules and less.<sup>80</sup> Larger chains are interrupted too frequently, allowing only a stepwise mechanism, even if the interruptions are of transient nature.

### 3. CONCLUSION

In this work, we have elucidated structural and dynamical characteristics of water wires of typical length and time scales of 5–15 Å and 2–4 ps, respectively. The concept of water wires is a controversial matter, partially due to a lack of well-defined quantitative criteria but also due to uncertainties regarding the microscopic understanding of the corresponding relevant molecular motion.

We have addressed this issue by looking at the hydrogen bond network (and its dynamics) between two well-defined geometric sites, which are represented by the hydrogen bond donor and acceptor sites of two specific photoacid/-base chromophores from the hydroxyquinoline family (6- and 7HQ). Both exist in two rotamers, yielding a total of four initial/final coordinates for a water wire. Such photoacids/-bases are of particular interest because transient time-dependent femtosecond IR spectroscopy can provide spectroscopic fingerprints of intermediate conformations during a

proton transfer process initiated by electronic excitation. These intermediate structures provide experimental evidence for the existence, persistence, and relevance of water wires between the donor/acceptor sites.

Different topologies of possible protonation pathways are discriminated by their geometric properties, in particular the number of water molecules. Our *ab initio* molecular dynamic simulations showed that the water wire patterns for the *cis* conformation are more stable than the *trans* conformers. We found that *cis*-7HQ can indeed establish short water wires consisting of three to six molecules, which can accelerate proton exchange reactions by lowering the reaction barrier, favoring a concerted proton transfer reaction. For other HQ derivatives, the length of the water wires is larger (five molecules and more), which would yield a stepwise proton transfer process.

Our molecular dynamics simulations provide a consistent picture of hydrogen bonded chains between well-defined sites of solvated photoacids/-bases. The present study provides elements to reconcile the transient water wire motifs with a detailed atomistic picture of hydrogen bonding in aqueous bulk solutions. Our results provide a sound microscopic basis for the interpretation of femtosecond transient fluorescence and IR experiments in terms of the water wire concept.

### ■ ASSOCIATED CONTENT

#### 📄 Supporting Information

Computational details and characterization data for the simulations. This material is available free of charge via the Internet at <http://pubs.acs.org>.

### ■ AUTHOR INFORMATION

#### Corresponding Author

\*E-mail: [daniel.sebastiani@chemie.uni-halle.de](mailto:daniel.sebastiani@chemie.uni-halle.de).

#### Notes

The authors declare no competing financial interest.

### ■ ACKNOWLEDGMENTS

The computing infrastructure was provided by the NIC supercomputers of the Research Centre Jülich. This work was

supported by Leibniz Graduate School of Molecular Biophysics Berlin and German Research Foundation (DFG) under grant SE 1008/11-1.

## REFERENCES

- (1) Hayes, R. L.; Paddison, S. J.; Tuckerman, M. E. Proton Transport in Triflic Acid Hydrates Studied via Path Integral Car-Parrinello Molecular Dynamics. *J. Phys. Chem. B* **2009**, *113*, 16574–16589.
- (2) Mohammed, O. F.; Pines, D.; Nibbering, E. T. J.; Pines, E. Base-induced solvent switches in acid-base reactions. *Angew. Chem.* **2007**, *119*, 1480–1483.
- (3) Hynes, J. T. Physical chemistry: the peripatetic proton. *Nature* **2007**, *446*, 270–273.
- (4) Rini, M.; Magnes, B.-Z.; Pines, E.; Nibbering, E. T. J. Real-time observation of bimodal proton transfer in acid-base pairs in water. *Science* **2003**, *301*, 249–352.
- (5) Mohammed, O. F.; Pines, D.; Nibbering, E. T. J.; Pines, E. Base-induced solvent switches in acid-base reactions. *Angew. Chem.* **2007**, *119*, 1480–1483.
- (6) Adamczyk, K.; Prémont-Schwarz, M.; Pines, D.; Pines, E.; Nibbering, E. T. J. Real-time observation of carbonic acid formation in aqueous solution. *Science* **2009**, *326*, 1690–1694.
- (7) Bodi, A.; Csontos, J.; Kallay, M.; Borkar, S.; Sztaray, B. On the protonation of water. *Chem. Sci.* **2014**, *5*, 3057–3063.
- (8) Laage, D.; Hynes, J. T. A Molecular Jump Mechanism of Water Reorientation. *Science* **2006**, *311*, 832–835.
- (9) Elgabarty, H.; Schmieder, P.; Sebastiani, D. Unraveling the existence of dynamic water channels in light-harvesting proteins: Alpha-C-phycocyanobilin in vitro. *Chem. Sci.* **2013**, *4*, 755–763.
- (10) Raghavender, U. S.; Kantharaju; Aravinda, S.; Shamala, N.; Balaran, P. Hydrophobic Peptide Channels and Encapsulated Water Wires. *J. Am. Chem. Soc.* **2010**, *132*, 1075–1086.
- (11) Olschewski, M.; Knop, S.; Lindner, J.; Vöhringer, P. From Single Hydrogen Bonds to Extended Hydrogen-Bond Wires: Low-Dimensional Model Systems for Vibrational Spectroscopy of Associated Liquids. *Angew. Chem., Int. Ed.* **2013**, *52*, 9634–9654.
- (12) Garczarek, F.; Gerwert, K. Functional waters in intraprotein proton transfer monitored by FTIR difference spectroscopy. *Nature* **2006**, *439*, 109–112.
- (13) Heim, R.; Cubitt, A.; Tsien, R. Improved green fluorescence. *Nature* **1995**, *373*, 663–664.
- (14) Chalfie, M.; Tu, Y.; Euskirchen, G.; Ward, W.; Prasher, D. Improved green fluorescence. *Science* **1994**, *263*, 802–805.
- (15) Cui, Q.; Karplus, M. Is “proton wire” concerted or step-wise? A model study of proton transfers in carbonic anhydrase. *J. Phys. Chem. B* **2003**, *107*, 1071–1078.
- (16) Yu, C.; Cukierman, S.; Pomés, R. Theoretical study of the structure and dynamic fluctuations of dioxolane-linked gramicidin channels. *Biophys. J.* **2003**, *84*, 816–831.
- (17) Villabona-Monsalve, J. P.; Islas, R. E.; Rodríguez-Córdoba, W.; Matsika, S.; Peón, J. Ultrafast Excited State Dynamics of Allopurinol, a Modified DNA Base. *J. Phys. Chem. A* **2013**, *117*, 898–904.
- (18) Dedecker, P.; de Schryver, F. C.; Hofkens, J. Fluorescent Proteins: Shine on, You Crazy Diamond. *J. Am. Chem. Soc.* **2013**, *135*, 2387–2402.
- (19) Dumat, B.; Bordeau, G.; Faurel-Paul, E.; Mahuteau-Betzer, F.; Saettel, N.; Metge, G.; Fiorini-Debuisschert, C.; Charra, F.; Teulade-Fichou, M.-P. DNA Switches on the Two-Photon Efficiency of an Ultrabright Triphenylamine Fluorescent Probe Specific of AT Regions. *J. Am. Chem. Soc.* **2013**, *135*, 12697–12706.
- (20) Allolio, C.; Sajadi, M.; Ernsting, N.; Sebastiani, D. An Ab Initio Microscope: Molecular Contributions to the Femtosecond Time-Dependent Fluorescence Shift of a Reichardt-Type Dye. *Angew. Chem., Int. Ed.* **2013**, *52*, 1813–1816.
- (21) Kim, T. G.; Topp, M. R. Ultrafast Excited-State Deprotonation and Electron Transfer in Hydroxyquinoline Derivatives. *J. Phys. Chem. A* **2004**, *108*, 10060–10065.
- (22) Gould, E.-A.; Popov, A. V.; Tolbert, L. M.; Presiado, I.; Erez, Y.; Huppert, D.; Solntsev, K. M. Excited-state proton transfer in N-methyl-6-hydroxyquinolinium salts: solvent and temperature effects. *Phys. Chem. Chem. Phys.* **2012**, *14*, 8964–8973.
- (23) Veiga-Gutiérrez, M.; Brenlla, A.; Carreira Blanco, C.; Fernández, B.; Kovalenko, S. A.; Rodríguez-Prieto, F.; Mosquera, M.; Lustres, J. L. P. Dissociation of a Strong Acid in Neat Solvents: Diffusion Is Observed after Reversible Proton Ejection Inside the Solvent Shell. *J. Phys. Chem. B* **2013**, *117*, 14065–14078.
- (24) Bardez, E.; Boutin, P.; Valeur, B. Photoinduced biprotonic transfer in 4-methylumbelliferone. *Chem. Phys. Lett.* **1992**, *191*, 142–148.
- (25) Krauter, C. M.; Mohring, J.; Buckup, T.; Pernpointner, M.; Motzkus, M. Ultrafast branching in the excited state of coumarin and umbelliferone. *Phys. Chem. Chem. Phys.* **2013**, *15*, 17846–17861.
- (26) Kwon, O.; Lee, Y.; Yoo, B. K.; Jang, D. ExcitedState Triple Proton Transfer of 7-Hydroxyquinoline along a HydrogenBonded Alcohol Chain: Vibrationally Assisted Proton Tunneling. *Angew. Chem.* **2006**, *118*, 429–433.
- (27) Park, S.-Y.; Lee, Y.-S.; Kwon, O.-H.; Jang, D.-J. Proton transport of water in acid-base reactions of 7-hydroxyquinoline. *Chem. Commun.* **2009**, 926–928.
- (28) Park, S.-Y.; Kim, B.; Lee, Y.-S.; Kwon, O.-H.; Jang, D.-J. Triple proton transfer of excited 7-hydroxyquinoline along a hydrogen-bonded water chain in ethers: secondary solvent effect on the reaction rate. *Photochem. Photobiol. Sci.* **2009**, *8*, 1611–1617.
- (29) Kwon, O.-H.; Mohammed, O. F. Water-wire catalysis in photoinduced acid-base reactions. *Phys. Chem. Chem. Phys.* **2012**, *14*, 8974–8980.
- (30) Bach, A.; Hewel, J.; Leutwyler, S. Hydrogen Bonding and Intermolecular Vibrations of 6-HydroxyquinolineH<sub>2</sub>O in the S<sub>0</sub> and S<sub>1</sub> States. *J. Phys. Chem. A* **1998**, *102*, 10476–10485.
- (31) Bach, A.; Leutwyler, S. Water-chain clusters: vibronic spectra of 7-hydroxyquinoline(H<sub>2</sub>O)<sub>n</sub>, n=1–4. *Chem. Phys. Lett.* **1999**, *299*, 381–388.
- (32) Bach, A.; Coussan, S.; Müller, A.; Leutwyler, S. Water-wire clusters: Vibronic spectra of 7-hydroxyquinoline(H<sub>2</sub>O)<sub>3</sub>. *J. Chem. Phys.* **2000**, *113*, 9032–9043.
- (33) Manca, C.; Tanner, C.; Coussan, S.; Bach, A.; Leutwyler, S. H atom transfer along an ammonia chain: tunneling and mode selectivity in 7-hydroxyquinoline.(NH<sub>3</sub>)<sub>3</sub>. *J. Chem. Phys.* **2004**, *121*, 2578–2590.
- (34) Tanner, C.; Manca, C.; Leutwyler, S. Exploring excited-state hydrogen atom transfer along an ammonia wire cluster: Competitive reaction paths and vibrational mode selectivity. *J. Chem. Phys.* **2005**, *122*, 204326.
- (35) Tanner, C.; Thut, M.; Steinlin, A.; Manca, C.; Leutwyler, S. Excited-state hydrogen-atom transfer along solvent wires: Water molecules stop the transfer. *J. Phys. Chem. A* **2005**, *110*, 1758–1766.
- (36) Tanner, C.; Manca, C.; Leutwyler, S. Probing the Threshold to H Atom Transfer Along a Hydrogen-Bonded Ammonia Wire. *Science* **2003**, *302*, 1736–1739.
- (37) Liu, Y. H.; Mehata, M. S.; Liu, J. Y. Excited-state proton transfer via hydrogen-bonded acetic acid (AcOH) wire for 6-hydroxyquinoline. *J. Phys. Chem. A* **2011**, *115*, 19–24.
- (38) Mehata, M. S. Proton translocation and electronic relaxation along a hydrogen-bonded molecular wire in a 6-hydroxyquinoline/acetic acid complex. *J. Phys. Chem. B* **2008**, *112*, 8383–8386.
- (39) Fernández-Ramos, A.; Martínez-Núñez, E.; Vázquez, S. A.; Ríos, M. A.; Estévez, C.; Merchán, M.; Serrano-Andrés, L. Hydrogen transfer vs proton transfer in 7-hydroxy-quinoline.(NH<sub>3</sub>)<sub>3</sub>: a CASSCF/CASPT2 study. *J. Phys. Chem. A* **2007**, *111*, 5907–5912.
- (40) Bekçioglu, G.; Allolio, C.; Ekimova, M.; Nibbering, E. T. J.; Sebastiani, D. Competition between excited state proton and OH-transport via a short water wire: solvent effects open the gate. *Phys. Chem. Chem. Phys.* **2014**, *16*, 13047–13051.
- (41) Pérez-Lustres, J. L.; Rodríguez-Prieto, F.; Mosquera, M.; Senyushkina, T. A.; Ernsting, N. P.; Kovalenko, S. A. *J. Am. Chem. Soc.* **2007**, *129*, 5408–5418.



- (42) Konijnenberg, J.; Ekelmans, G. B.; Huizer, A. H.; Varma, C. A. G. O. Mechanism and solvent dependence of the solvent-catalysed pseudo-intramolecular proton transfer of 7-hydroxyquinoline in the first electronically excited singlet state and in the ground state of its tautomer. *J. Chem. Soc., Faraday Trans. 2* **1989**, *85*, 39–51.
- (43) Bhattacharya, B.; Samanta, A. Excited-State Proton-Transfer Dynamics of 7-Hydroxyquinoline in Room Temperature Ionic Liquids. *J. Phys. Chem. B* **2008**, *112*, 10101–10106.
- (44) Lim, H.; Jeong, H.; Park, S.-Y.; Lee, J. Y.; Jang, D.-J. Excited-state proton-relay dynamics of 7-hydroxyquinoline controlled by solvent reorganization in room temperature ionic liquids. *Phys. Chem. Chem. Phys.* **2012**, *14*, 218–224.
- (45) Abou-Zied, O. K.; Husband, J.; Al-Lawatia, N.; Steinbrecher, T. B. Ground state spectroscopy of hydroxyquinolines: evidence for the formation of protonated species in water-rich dioxane-water mixtures. *Phys. Chem. Chem. Phys.* **2014**, *16*, 61–70.
- (46) Park, S.-Y.; Lee, Y.-S.; Jang, D.-J. Ground-state proton-transfer dynamics governed by configurational optimization. *Phys. Chem. Chem. Phys.* **2011**, *13*, 3730–3736.
- (47) VandeVondele, J.; Mohamed, F.; Krack, M.; Hutter, J.; Sprik, M.; Parrinello, M. The influence of temperature and density functional models in ab initio molecular dynamics simulation of liquid water. *J. Chem. Phys.* **2005**, *122*, 014515.
- (48) Grimme, S. Semiempirical GGA-type density functional constructed with a long-range dispersion correction. *J. Comput. Chem.* **2006**, *27*, 1787–1799.
- (49) Lippert, G.; Hutter, J.; Parrinello, M. A hybrid Gaussian and plane wave density functional scheme. *Mol. Phys.* **1997**, *92*, 477–487.
- (50) Hutter, J.; Iannuzzi, M.; Schiffmann, F.; VandeVondele, J. Computer code CP2K. CP2K.org.
- (51) Schäfer, A.; Huber, C.; Ahlrichs, R. Fully optimized contracted Gaussian-basis sets of triple zeta valence quality for atoms Li to Kr. *J. Chem. Phys.* **1994**, *100*, 5829–5835.
- (52) Goedecker, S.; Teter, M.; Hutter, J. Separable Dual-Space Gaussian Pseudopotentials. *Phys. Rev. B* **1996**, *54*, 1703–1710.
- (53) Frisch, M. J.; Trucks, G. W.; Schlegel, H. B.; Scuseria, G. E.; Robb, M. A.; Cheeseman, J. R.; Scalmani, G.; Barone, V.; Mennucci, B.; Petersson, G. A.; et al. *Gaussian 09*, revision A.02; Gaussian, Inc.: Wallingford, CT, 2009.
- (54) Becke, A. D. Density-functional thermochemistry. 3. The role of exact exchange. *J. Chem. Phys.* **1993**, *8*, 5648–5652.
- (55) Barone, V.; Cossi, M. Quantum calculation of molecular energies and energy gradients in solution by a conductor solvent model. *J. Phys. Chem. A* **1998**, *102*, 1995–2001.
- (56) Luzar, A.; Chandler, D. Effect of Environment on Hydrogen Bond Dynamics in Liquid Water. *Phys. Rev. Lett.* **1996**, *76*, 928–931.
- (57) Agmon, N. Elementary steps in excited-state proton transfer. *J. Phys. Chem. A* **2005**, *109*, 13–35.
- (58) Schiffmann, C.; Sebastiani, D. Hydrogen bond networks: Structure and dynamics via first-principles spectroscopy. *Phys. Status Solidi B* **2012**, *249*, 368–375.
- (59) Allolio, C.; Salas-Illanes, N.; Desmukh, Y. S.; Hansen, M. R.; Sebastiani, D. H-Bonding Competition and Clustering in Aqueous LiI. *J. Phys. Chem. B* **2013**, *117*, 9939–9946.
- (60) Brehm, M.; Kirchner, B. TRAVIS - A Free Analyzer and Visualizer for Monte Carlo and Molecular Dynamics Trajectories. *J. Chem. Inf. Model.* **2011**, *51*, 2007–2023.
- (61) Laage, D.; Stirnemann, G.; Hynes, J. T. Why Water Reorientation Slows without Iceberg Formation around Hydrophobic Solutes. *J. Phys. Chem. B* **2009**, *113*, 2428–2435.
- (62) Laage, D.; Stirnemann, G.; Sterpone, F.; Rey, R.; Hynes, J. T. Reorientation and Allied Dynamics in Water and Aqueous Solutions. *Annu. Rev. Phys. Chem.* **2011**, *62*, 395–416.
- (63) de Grotthuss, C. J. T. Sur la décomposition de l'eau et des corps qu'elle tient en dissolution à l'aide de l'électricité galvanique. *Ann. Chim.* **1806**, *58*, 54–73.
- (64) Danneel, V. H. Notiz über ionengeschwindigkeiten. *Z. Elektrochem.* **1905**, *11*, 249–252.
- (65) Agmon, N. The Grotthuss mechanism. *Chem. Phys. Lett.* **1995**, *244*, 456–462.
- (66) Morrone, J. A.; Tuckerman, M. E. Ab initio molecular dynamics study of proton mobility in liquid methanol. *J. Chem. Phys.* **2002**, *117*, 4403–4413.
- (67) Izvekov, S.; Voth, G. A. Ab initio molecular-dynamics simulation of aqueous proton solvation and transport revisited. *J. Chem. Phys.* **2005**, *123*, 44505.
- (68) Geissler, P.; Dellago, C.; Chandler, D.; Hutter, J.; Parrinello, M. Ab initio analysis of proton transfer dynamics in (H<sub>2</sub>O)<sub>3</sub>H<sup>+</sup>. *Chem. Phys. Lett.* **2000**, *321*, 225–230.
- (69) Hassanali, A. A.; Cuny, J.; Ceriotti, M.; Pickard, C. J.; Parrinello, M. The fuzzy quantum proton in the hydrogen chloride hydrates. *J. Am. Chem. Soc.* **2012**, *134*, 8557–8569.
- (70) Hassanali, A.; Prakash, M. K.; Eshet, H.; Parrinello, M. On the recombination of hydronium and hydroxide ions in water. *Proc. Natl. Acad. Sci. U.S.A.* **2011**, *108*, 20410–20415.
- (71) Hassanali, A.; Giberti, F.; Cuny, J.; Kühne, T. D.; Parrinello, M. Proton transfer through the water gossamer. *Proc. Natl. Acad. Sci. U.S.A.* **2013**, *110*, 13723–13728.
- (72) Mei, H. S.; Tuckerman, M. E.; Sagnella, D. E.; Klein, M. L. Quantum Nuclear ab Initio Molecular Dynamics Study of Water Wires. *J. Phys. Chem. B* **1998**, *102*, 10446–10458.
- (73) Sadeghi, R. R.; Cheng, H.-P. The dynamics of proton transfer in a water chain. *J. Chem. Phys.* **1999**, *111*, 2086–2094.
- (74) Fecko, C. J.; Eaves, J. D.; Loparo, J. J.; Tokmakoff, A.; Geissler, P. L. Ultrafast Hydrogen-Bond Dynamics in the Infrared Spectroscopy of Water. *Science* **2003**, *301*, 1698–1702.
- (75) Eaves, J. D.; Loparo, J. J.; Fecko, C. J.; Roberts, S. T.; Tokmakoff, A.; Geissler, P. L. Hydrogen bonds in liquid water are broken only fleetingly. *Proc. Natl. Acad. Sci. U.S.A.* **2005**, *102*, 13019–13022.
- (76) Kühne, T. D.; Khaliullin, R. Z. Electronic signature of the instantaneous asymmetry in the first coordination shell of liquid water. *Nat. Commun.* **2013**, *4*, 1450.
- (77) Kühne, T. D.; Khaliullin, R. Z. Nature of the Asymmetry in the Hydrogen-Bond Networks of Hexagonal Ice and Liquid Water. *J. Am. Chem. Soc.* **2014**, *136*, 3395–3399.
- (78) Mohammed, O. F.; Pines, D.; Dreyer, J.; Pines, E.; Nibbering, E. T. J. Sequential proton transfer through water bridges in acid-base reactions. *Science* **2005**, *310*, 83–86.
- (79) Park, S.-Y.; Jang, D.-J. Accumulated Proton-Donating Ability of Solvent Molecules in Proton Transfer. *J. Am. Chem. Soc.* **2010**, *132*, 297–302.
- (80) Cox, M. J.; Timmer, R. L. A.; Bakker, H. J.; Park, S.; Agmon, N. Distance-Dependent Proton Transfer along Water Wires Connecting Acid–Base Pairs. *J. Phys. Chem. A* **2009**, *113*, 6599–6606.